

Morphology and Properties of Soy Protein Plastics Modified with Chitin

Hua Zheng,¹ Zhan'ao Tan,¹ Yuan Ran Zhan,² Jin Huang³

¹Department of Chemical Engineering, Wuhan University of Technology, Wuhan 430070, People's Republic of China

²State Key Laboratory of Advanced Technology for Materials Synthesis and Processing, Wuhan University of Technology, Wuhan 430070, People's Republic of China

³Department of Chemistry, Wuhan University, Wuhan 430072, People's Republic of China

Received 3 December 2002; accepted 2 April 2002

ABSTRACT: A series of bioplastics from isolated soy protein (SPI) and chitin (CH) was prepared with glycerol as a plasticizer by blending and compression molding. Their morphology and properties were investigated by wide-angle X-ray diffraction (WAXD), differential scanning calorimetry (DSC), dynamical mechanical thermal analysis (DMTA), scanning electron microscopy (SEM), and tensile and water-absorption tests. The added CH as a filler cannot strongly interact with SPI molecules and, hence, this results in phase separation in blends. However, the rigid nature of the CH molecules enhanced the tensile strength and Young's

modulus, but decreased the breaking elongation of the materials. When the CH content was higher than 10 wt %, the water absorption of the blends were obviously lower than that of the sheets without CH, resulting from the formation of a CH framework in the blends. Both soy protein and CH exhibit good biodegradability, biocompatibility, and bioactivity, and their composites may become a promising biomaterial. © 2003 Wiley Periodicals, Inc. *J Appl Polym Sci* 90: 3676–3682, 2003

Key words: blends; phase separation

INTRODUCTION

Plastics made from abundant and low-cost soy protein have been evaluated as potential substitutes for petroleum-based plastics due to their renewable, biodegradable, environmentally friendly features. Thus, more and more attention has been given to the development of soy protein plastics using the processes of compression molding, injection molding, and screw-extrusion.^{1–4} However, soy protein plastics are very rigid and brittle and have water sensitivity. Therefore, many chemical and physical modifications have been explored to improve the processibility, mechanical properties, and water resistance of soy protein-based materials, such as acetylation,⁵ esterification,⁶ and denaturation⁷ of soy protein, guanidine hydrochloride⁸ and sodium dodecyl sulfate modification,⁹ incorporation of a filler,^{10,11} and blending with other biodegradable polymers.^{12–14}

Blending is an important method in polymer manufacture and has received increasing attention because of strong economic and academic incentives for the development of polymeric materials. Many efforts have been made to blend soy protein with biodegradable synthetic polymers and to improve the properties of blends by compatibilization. A polyphosphate filler

was introduced into soy protein plastics to improve the mechanical properties and water resistance.¹⁰ Blend plastics from soy protein and anhydride-modified polyester were prepared by injection molding, which exhibited good miscibility and, hence, enhanced the mechanical strength and the moisture sensitivity.¹² Soy protein/polycaprolactone (PCL) compatibilized by methylene diphenyl diisocyanate (MDI) was melt-blended and then compression-molded. The introduction of PCL enhanced the breaking elongation, toughness, and water resistance of the materials, but decreased the tensile strength and Young's modulus, while the compatibilization by MDI further improved the mechanical properties and restricted water absorption.¹³ The soy protein plastic was modified by biomax/poly(vinyl alcohol) (PVA) and biomax/PCL and compatibilized with polyvinylactam (PVL) by the processes of extrusion and injection-molding. The blends demonstrated high strength and modulus but brittle characteristics, and the strength increased with increase of the polymer concentration. PVL worked well as a compatibilizer for the blends, and the synthetic polymer was effective for reducing the moisture sensitivity of the soy protein.¹⁴

However, the high cost of biodegradable synthetic polymers has hindered the wide application of blend plastics based on soy protein. Thus, the abundant and low-cost natural polysaccharides were blended into the soy protein-based materials by virtue of their reactive and derivative characteristics. Starch is a ther-

Correspondence to: Z. Tan.

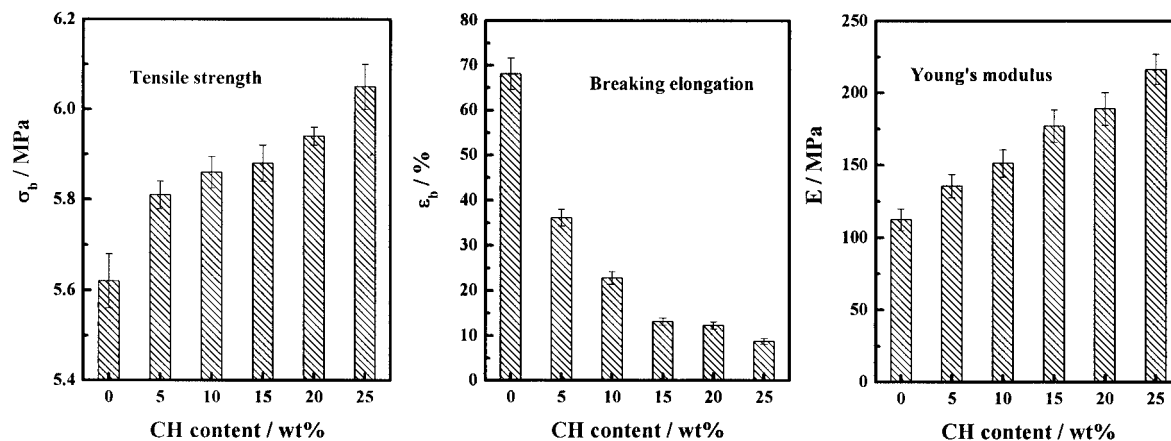


Figure 1 Tensile strength (σ_b), breaking elongation (ϵ_b), and Young's modulus (E) of the SP-C sheets with various CH contents.

moplastic polymeric material that is used widely to modify soy protein plastics. The blend starch/soy protein plastics could be extruded and injection-molded into articles of various shapes and sizes, and the products had good tensile properties and water resistance.^{15,16} Long-fiber, short-fiber, and microcrystalline cellulose were incorporated as a filler into soy protein plastics at various levels.¹¹ Rigid cellulose molecules lowered the breaking elongation of the materials, but enhanced the rigidity and slightly improved the water absorption. In addition, lignosulfonate was introduced into soy protein plastics by blending and hot pressing and, hence, it interacted with the soy protein molecules to form networks with physical crosslinks, resulting in the enhancement of the mechanical properties and water sensitivity of soy protein-based materials.¹⁷ At the same time, alkaline lignin, with a hydrophobic nature, was also blended into soy protein plastics, resulting in improvement of the tensile strength and water sensitivity.¹⁸

Chitin (CH), the second abundant natural polymer, is a hard, inelastic, and nitrogenous polysaccharide, and its structure is similar to cellulose except for an acetamido group at position C-2. CH is recommended as a suitable functional material due to its excellent biocompatibility, biodegradability, nontoxicity, reactivity, etc.¹⁹ Thus, it would be beneficial to modify soy protein plastics with CH to improve the properties of materials. In this work, a soy protein isolated/CH sheet was obtained by blending in an intensive mixer and compression molding. The effects of CH on the morphology and properties of soy protein plastics were investigated by wide-angle X-ray diffraction (WAXD), differential scanning calorimetry (DSC), dynamical mechanical thermal analysis (DMTA), scanning electron microscopy (SEM), and tensile and water-absorption tests.

EXPERIMENTAL

Materials and preparation of samples

Soy protein isolate (SPI) with moisture content of 6.8% was provided by the Yunmeng Protein Technologies Co. (Hubei, China) and used without further treatment. CH was supplied by the Yuhuan Ocean Biochemistry Co. (Zhejiang, China). Glycerol (GL), analytical grade, was purchased from the Shanghai Chemical Co. (Shanghai, China).

The mixtures of SPI and 0, 5, 10, 15, 20, and 25 wt % CH with the addition of 30 wt % GL were mechanically mixed at room temperature, followed by melt blending with an intensive mixer (Brabender Instruments Co., Germany) at 140°C and 30 rpm for 8 min. Subsequently, the blend was placed in a mold covered with two polished stainless-steel plates and then compression-molded using a hot-press. The specimen was molded at 160°C and 20 MPa for 5 min and then wind-cooled to about 50°C for 0.5 h under constant pressure before removal from the mold to obtain the blend sheets. All the sheets were coded as SP-C0–SP-C5 according to the CH content from 0 to 25 wt %.

Characterization

WAXD patterns of the sheets were recorded on a D/max-1200 X-ray diffractometer (Rigaku Denki, Japan) with $\text{CuK}\alpha$ radiation ($\lambda = 1.5405 \times 10^{-10}$ m). The samples were examined with 2θ ranging from 4 to 60° at a scanning rate of $10^\circ \text{ min}^{-1}$.

SEM micrographs were taken on an S-570 SEM microscope (Hitachi, Japan). The sheets were frozen in liquid nitrogen and then vacuum-dried followed by snapping. The cross sections of the sheets were coated with gold for SEM observation.

The tensile strength (σ_b), breaking elongation (ϵ_b), and Young's modulus (E) of the sheets were measured

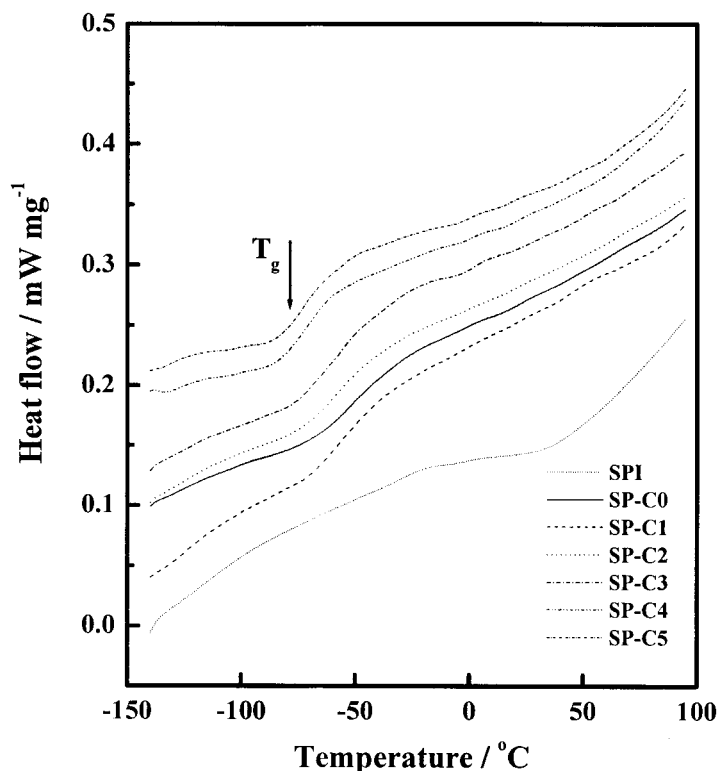


Figure 2 DSC thermograms of the SP-C sheets with various CH contents.

on a CMT6503 universal testing machine (Shenzhen SANS Test Machine Co. Ltd., China) with a tensile rate of 10 mm min^{-1} according to ISO6239-1986 (E). DSC was performed on a DSC-204 apparatus (Netzsch Co., Germany) under a nitrogen atmosphere at a rate of $10^\circ\text{C min}^{-1}$ from -140 to 95°C . Prior to the test, the samples were heated from the room temperature to 100°C and then cooled to -150°C at a rate of $20^\circ\text{C min}^{-1}$.

DMTA was carried out using a DMTA-V dynamic mechanical analyzer (Rheometric Scientific Co., USA) at a frequency of 1 Hz. The temperature ranged from -110 to 150°C with a heating rate of 5°C min^{-1} . Thermogravimetric analysis (TGA) curves of the sheets were recorded on a TG 209 thermoanalyzer (Netzsch Co., Germany) under a nitrogen atmosphere from 25 to 800°C at a heating rate of $10^\circ\text{C min}^{-1}$.

Water absorption

Water absorption was measured, according to the ASTM standard D570-81 with minor modification. The samples were vacuum-dried for 72 h and then dried at 50°C for 24 h in an oven. Subsequently, they were cooled in a desiccator for a few minutes, weighed, and submerged in distilled water at room temperature for 26 h. The extra water on the surface of a specimen after water soaking was removed with a paper towel, and the specimen then was weighed

again. The container without the soaking specimen was placed in an air oven at 50°C for 72 h to evaporate the water, and the water-soluble content equals the increase of the container weight. The water absorption (Ab) was calculated by the following:

$$Ab = (W_1 - W_0 + W_{\text{sol}})/W_0$$

where W_1 , W_0 , and W_{sol} are the weight of the specimen containing water, the weight of the dried specimen, and the weight of water-soluble residuals, respectively.

TABLE I
DSC Data and the Crystalline Degree
for the SP-C Sheets and SPI

Sample	Glass transition		χ_c (%)
	T_g (onset) ($^\circ\text{C}$)	ΔC_p ($\text{J g}^{-1} \text{K}^{-1}$)	
SPI	—	—	0.31
CH	—	—	0.81
SP-C0	-67.6	0.25	0.41
SP-C1	-69.2	0.24	0.42
SP-C2	-71.9	0.26	0.45
SP-C3	-76.7	0.40	0.48
SP-C4	-83.0	0.29	0.50
SP-C5	-83.3	0.33	0.52

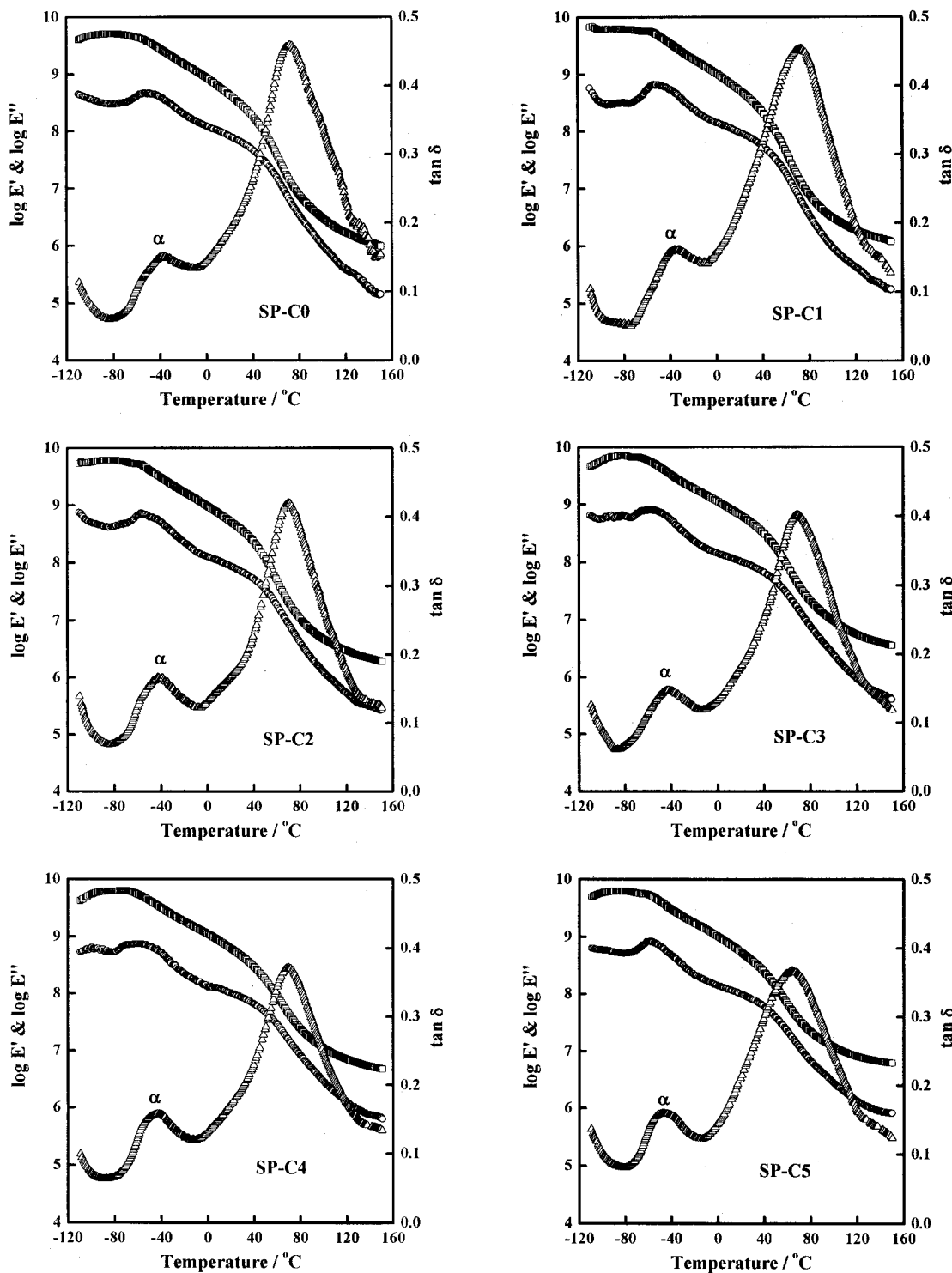


Figure 3 Storage modulus ($\log E'$), loss modulus ($\log E''$), and $\tan \delta$ as functions of temperature for the SP-C sheets.

RESULTS AND DISCUSSION

Mechanical properties

The effects of the CH content on the tensile strength (σ_b), breaking elongation (ϵ_b), and Young's modulus (E) for the SP-C sheets are shown in Figure 1. The incorporation of CH, similar to cellulose, decreased

the breaking elongation, but increased the tensile strength and rigidity of the materials, resulting from the rigid nature of the CH molecules. With increase of the CH content, the σ_b and E of the materials increased while the ϵ_b decreased, suggesting that the increase of the CH content expanded the extent of phase separation. The enhancement of the strength may result from

TABLE II
DMTA Data of the SP-C Sheets

Sample	α -Relaxation				Loss peak	
	$T_{\alpha,1}$ (°C)	Log E''	$T_{\alpha,2}$ (°C)	$\tan \delta$	T_{\max} (°C)	$\tan \delta$
SP-C0	-53.42	8.675	-36.15	0.152	72.93	0.460
SP-C1	-53.88	8.827	-36.17	0.161	72.85	0.454
SP-C2	-56.69	8.845	-42.39	0.167	70.66	0.420
SP-C3	-57.15	8.851	-42.69	0.148	69.86	0.401
SP-C4	-57.51	8.876	-43.56	0.137	69.74	0.371
SP-C5	-57.99	8.924	-46.98	0.160	63.41	0.367

$T_{\alpha,1}$ and $T_{\alpha,2}$ were obtained from the curves of log E'' and $\tan \delta$ versus temperature, respectively.

phase separation, but it is inevitable that phase separation damaged the elongation of the materials.

Thermal properties

DSC thermograms of the SP-C sheets are shown in Figure 2, and the glass transition temperature (T_g) and the change of the heat capacities (ΔC_p) are listed in Table I. The combination of the plasticization of GL and the compression process resulted in the evident glass transition attributed to SPI. All the SP-C sheets containing CH had a lower T_g than that of SP-C0 without CH, suggesting that the addition of CH aided the phase separation in the blends. At the same time, the increase of the CH content resulted in the shift of the T_g to lower temperature, indicating expansion of the extent of phase separation.

DMTA curves of the SP-C sheets are shown in Figure 3, and the related information is summarized in Table II. The slight increase of log E' at low temperature resulted mainly from the antiplasticization of GL to SPI, which stiffened the SPI molecules. Usually, the introduction of a filler may influence the log E' due to adhesion or the strong interaction of the components, but, here, the similar log E' values for all sheets indicated that poor interaction existed between SPI and CH. Usually, the T_g from the curves of log E'' and $\tan \delta$ versus temperature measured by DMTA, considered as T_{α} was higher than those measured from DSC due to the nature of the dynamic test. At the same time, the T_{α} from the log E'' - T curves was lower than that of the $\tan \delta$ - T curves. However, the T_{α} from the two kinds of curves was shifted to lower temperature with an increase of CH content, which confirmed the results of the DSC.

The $\tan \delta$ - T curves can usually be utilized to reveal information concerning molecular and/or segmental scale motions in polymers. The T_{α} of the SP-C sheets decreased with increase of the CH content, suggesting that the chain or segment of the SPI molecules can more freely move. It proved that the addition of CH resulted in phase separation in the materials and provided more space for the motion of molecular chains

or segments. At the same time, the increase of the CH content increased the extent of phase separation, which favored freedom of motion at the molecular level and resulted in the shift of T_{α} to low temperature with increase of the CH content.

Combined with the TGA curves shown in Figure 4, the loss peak at high temperature resulted from the thermodynamic relaxation of the materials, namely, the slow vaporization of GL and other volatile components. With increase of the CH content, the height of the loss peak decreased while the T_{\max} shifted to low temperature.

Crystallinity and morphology

The crystalline (χ_c) degree and WAXD patterns for SPI, CH, and SP-C sheets with different CH content are depicted in Table I and Figure 5, respectively. The increase of χ_c for the materials increased with increase of the CH content, suggesting the existence of phase

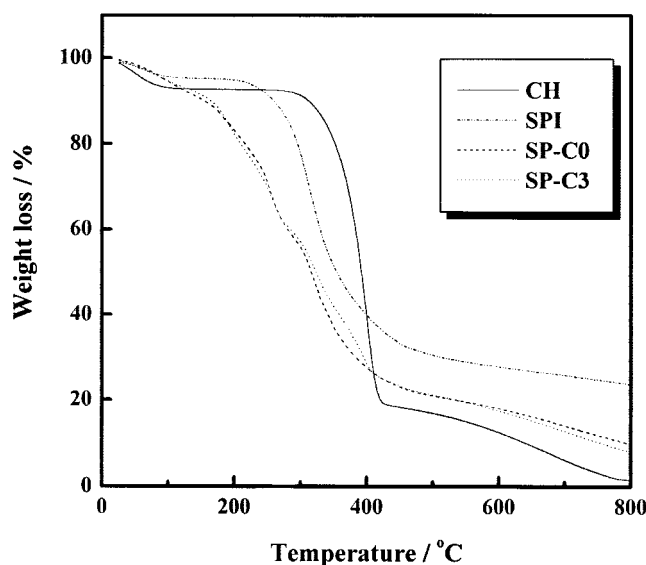


Figure 4 TGA curves of the sheets SP-C0 and SP-C3 and of CH and SPI.

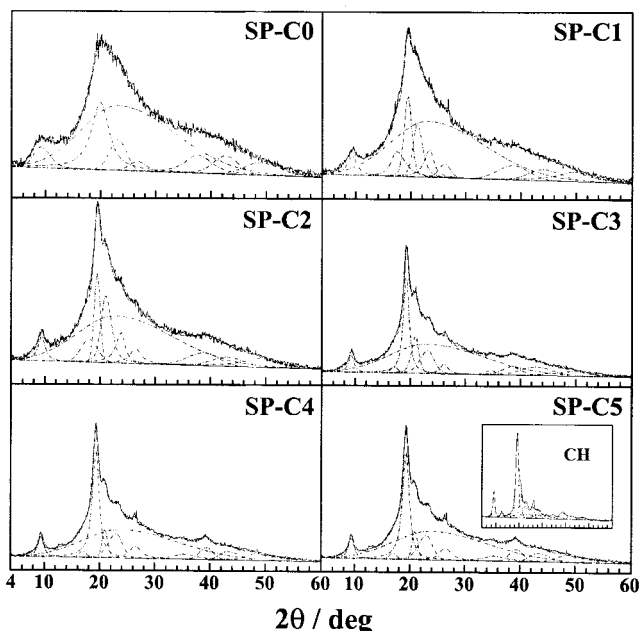


Figure 5 WAXD patterns of the SP-C sheets with various CH contents and CH and SPI.

separation. At the same time, the intensity of peak at about $2\theta = 19.3^\circ$ assigned to CH increased with increase of the CH content, indicating that CH existed in the materials independently due to the poor interaction between SPI and CH.

The cross sections of the SP-C sheets are shown in Figure 6. It is obvious that the SP-C sheets exhibited coarser cross sections than those of SP-C0 without the addition of CH, suggesting the existence of phase separation due to the addition of CH. At the same time, with increase of the CH content, the cross sections become coarser and coarser, indicating that the extent of phase separation expanded.

Water absorption

The effects of the CH content on the water absorption are shown in Figure 7. When the CH content in the materials was higher than 5 wt %, CH efficiently restricted the water absorption (*Ab*) of soy protein plastics. The rigid CH molecules can effectively restrict the swelling of soy protein plastics in water; thus, the water absorption decreased with an increase of the CH content. However, SP-C1 with 5 wt % CH exhibited higher water absorption than that of SP-C0 without CH, which resulted mainly from the existence of phase separation, which indicated poor interaction between the CH and SPI molecules.

Role of CH in the blends

The addition of CH did not strongly interact with the SPI molecules and, hence, resulted in phase separation

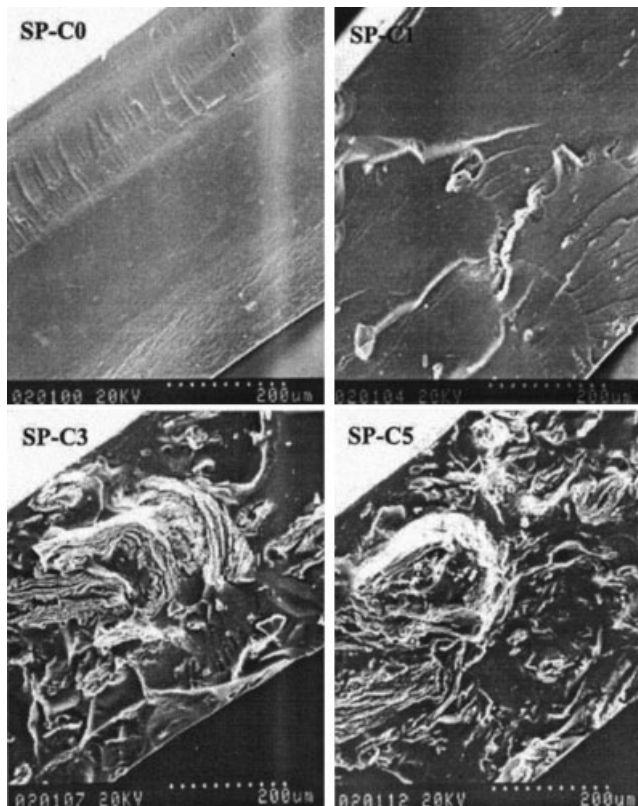


Figure 6 SEM images of the cross sections for the sheets SP-C0, SP-C1, SP-C3, and SP-C5.

of the blends. However, the rigidity of the CH molecules enhanced the strength and modulus of the blends and lowered the water absorption. Usually, the high water absorption of SPI sheets resulted mainly from its strong swelling ability. Thus, CH plays a key role in the blends as the framework of the whole

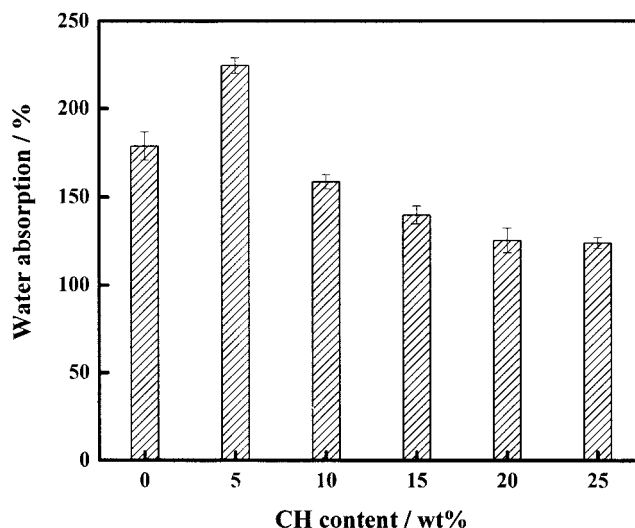


Figure 7 Effects of CH content on water absorption immersed in water for 26 h.

materials, which restricted the swelling of the materials.

CONCLUSIONS

A composite plastic based on SPI and CH was prepared by the plasticization of glycerol by blending and compression-molding. Although increase of the CH content resulted in enhancement of the tensile strength and Young's modulus, the incorporation of CH decreased the breaking elongation of the materials. When the CH content was higher than 10 wt %, the water absorption of SP-C sheets were obviously lower than that of SP-C0 without CH. The added CH cannot strongly interact with the SPI molecules and resulted in phase separation in the blends. The improvements of strength and modulus were attributed to the rigid nature of the CH molecules and the restriction of water absorption resulted from the formation of a CH framework for the blends.

References

1. Paetau, I.; Chen, C.; Jane, J. *Ind Eng Chem Res* 1994, 33, 1821.
2. Sue, H. J.; Wang, S.; Jane, J. *Polymer* 1997, 38, 5035.
3. Mo, X.; Sun, X. S.; Wang, Y. *J Appl Polym Sci* 1999, 73, 2595.
4. Zhang, J.; Mungara, P.; Jane, J. *Polymer* 2001, 42, 2569.
5. Foulk, J. A.; Bunn, J. M. *Ind Crops Prod* 2001, 14, 11.
6. Huang, H. M. S. Dissertation, Iowa State University, Ames, IA 1994.
7. Mo, X.; Sun, X. *JAOCS* 2001, 78, 867.
8. Zhong, Z. K.; Sun, X. S. *J Appl Polym Sci* 2000, 78, 1063.
9. Zhong, Z. K.; Sun, X. S. *J Appl Polym Sci* 2001, 81, 16.
10. Otaigbe, J. U.; Adams, D. O. *J Environ Polym Degrad* 1997, 5, 199.
11. Paetau, I.; Chen, C. Z.; Jane, J. *J Environ Polym Degrad* 1994, 2, 211.
12. John, J.; Bhattacharya, M. *Polym Int* 1999, 48, 1165.
13. Zhong, Z.; Sun, X. S. *Polymer* 2001, 42, 6961.
14. Mungara, P. M.; Chang, T.; Zhu, J.; Jane, J. *Polym Mater Sci Eng* 2002, 86, 364.
15. Otaigbe, J. U.; Jane, J. *J Environ Polym Degrad* 1997, 5, 75.
16. Park, S. K.; Hettiarachchy, N. S. *JAOCS* 1999, 76, 1201.
17. Huang, J.; Zhang, L. *J Appl Polym Sci*, in press.
18. Huang, J.; Zhang, L. *J Appl Polym Sci*, in press.
19. Ravi Kumar, M. N. V. *Rec Func Polym* 2000, 46, 1.